[6] *Immunogold-Silver Staining: Principles, Methods and Applications* (Ed.: M. A. Hayat), Academic Press, New York, **1995**.
[7] a) P. Eliades, E. Karagouni, I. Stergiaton, K. Kiras, *J. Immunol. Methods* **1998**, *210*, 123 – 132; b) G. Mayer, R. D. Leone, J. F. Hainfeld, M. Bendayan, *J. Histochem. Cytochem.* **2000**, *48*, 464 – 469.
[8] M. G. Sumi, A. Mathai, C. Sarada, V. V. Radhakrishnan, *J. Clin. Microbiol.* **1999**, *37*, 3925 – 3927.
[9] a) V. A. J. Kempf, K. Trebesius, I. B. Autenrieth, *J. Clin. Microbiol.* **2000**, *38*, 830 – 838; b) P. Kite, B. M. Dobbins, M. H. Wilcox, M. J. McMahon, *Lancet* **1999**, *354*, 1504 – 1507; c) P. V. Coyloe, A. Desai, D. Wyatt, C. McCaughey, H. E. O'Neil, *J. Virol. Methods* **1999**, *83*, 75 – 82.
[10] J. F. Hainfeld, F. R. Furuya, *Immunogold-Silver Staining: Principles, Methods and Applications*, (Ed.: M. A. Hayat), Academic Press, New York, **1995**, p. 92.
[11] K. R. Brown, M. J. Natan, *Langmuir* **1998**, *14*, 726 – 728.
[12] R. Rufner, N. E. Carson, M. Forte, G. Danscher, J. Gu, G. W. Hacker, *Cell Vision* **1995**, *2*, 327 – 333.
[13] $E = 1$ V versus NHE(Au) and $E_{1/2} = -0.4$ V versus NHE(NH_2OH); NHE = normal hydrogen electrode. A. J. Bard, *Encyclopedia of Electrochemistry of the Elements*, *Vol. 4*, Marcel Dekker, New York, **1975**.
[14] H. Perrot, J. R. Martin, P. J. Clechet, *J. Electrochem. Soc.* **1988**, *135*, 2881 – 2885.
[15] G. W. Hacker, G. Danscher, L. Grimelius, C. Hauser-Kronberger, W. H. Muss, A. Schiechl, J. Gu, O. Dietze. *Immunogold-Silver Staining: Principles, Methods and Applications*, (Ed.: M. A. Hayat), Academic Press, New York, **1995**, p. 29.
[16] T. Krenács, E. Molnár, E. Dobó, L. Dux, *Histochem. J.* **1989**, *21*, 145.
[17] a) G. Danscher, *Histochemistry* **1981**, *71*, 1 – 16; b) G. Danscher, *Histochemistry* **1981**, *71*, 81 – 88.
[18] G. W. Hacker, L. Grimelius, G. Danscher, G. Bernatzky, W. Muss, H. Adam, J. Thurner, *J. Histotechnol.* **1988**, *11*, 213 – 221.

Ligand Topology Tuning of Iron-Catalyzed Hydrocarbon Oxidations**

Miquel Costas and Lawrence Que, Jr.*

Nature has evolved a number of nonheme iron oxygenases capable of the stereoselective oxidation of C–H and C=C bonds.[1, 2] Still far from being understood are the factors that control the ability of iron centers to catalyze a range of reactions such as alkane hydroxylation, olefin epoxidation, and olefin *cis*-dihydroxylation. In our effort to develop bio-inspired nonheme iron catalysts, we have discovered a family of iron complexes with tetradentate pyridine/amine ligands that, in combination with H_2O_2, are capable of carrying out the above transformations with high stereoselectivity.[3–7] Enantioselectivity has also been obtained with the chiral ligand *N*,*N*′-bis(2-pyridylmethyl)-*N*,*N*′-dimethyl-*trans*-1,2-diaminocyclohexane (bpmcn).[8] A priori, tetradentate ligands with this type of architecture can adopt three different topologies (Scheme 1).[9–11] While Schiff's base ligands (e.g. salen) often afford complexes with the *trans* or planar

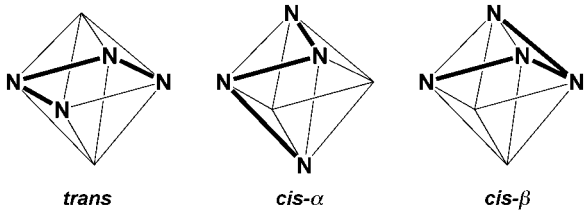

Scheme 1. Three different topologies that can be adopted by tetradentate ligands such as *N*,*N*′-bis(2-pyridylmethyl)-*N*,*N*′-dimethyl-*trans*-1,2-diaminocyclohexane (bpmcn).

topology, ligands such as bpmcn in which the imine functionalities have been reduced give rise to complexes with *cis*-α and/or *cis*-β topologies. We have undertaken a series of systematic studies to uncover the factors that control the catalytic reactivity of the nonheme iron center in this family of complexes.[5–7] Herein we report the unexpectedly distinct oxidation behavior of two [Fe^{II}(bpmcn)] catalysts, whose structures differ only by their ligand topologies.

[Fe^{II}(bpmcn)($OTf)_2$] (**1**, OTf = trifluoromethanesulfonate) complexes in both *cis*-α and *cis*-β ligand topologies can be synthesized by independent routes, and the structures of α-**1** and the related β-[Fe^{II}(5-Me_2-bpmcn)($OTf)_2$] have recently been established by crystallography.[8, 12] The NMR spectra of the two complexes strongly suggest that they each retain their respective ligand topologies in solution (Figure 1). Complex

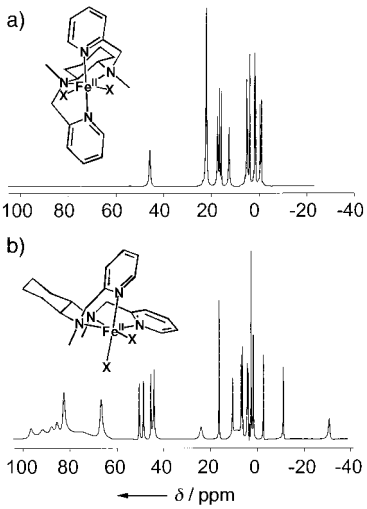

Figure 1. ^{1}H NMR spectra of α-[Fe^{II}(bpmcn)($CD_3CN)_2$]$^{2+}$ (a) and β-[Fe^{II}(bpmcn)($CD_3CN)_2$]$^{2+}$ (b) in CD_3CN solution at ambient temperature.

α-**1** exhibits 12 paramagnetically shifted signals, as expected for a C_2-symmetric high-spin Fe^{II} complex, while the β isomer shows 24 resonances. These isomers do not interconvert even after heating solutions of either isomer in acetonitrile at 50 °C for one day. The high barrier to interconversion arises from the fact that the N-methyl groups of the ligand have distinct

[*] Prof. Dr. L. Que, Jr., Dr. M. Costas
Department of Chemistry
and Center for Metals in Biocatalysis
University of Minnesota
207 Pleasant Street SE, Minneapolis, MN 55455 (USA)
Fax: (+1) 612-624-7029
E-mail: que@chem.umn.edu

[**] We thank the National Institutes of Health for financial support (GM33162 to L.Q.) and Fundacio La Caixa for a postdoctoral fellowship (M.C.).

  1433-7851/02/4112-2179 $ 20.00+.50/0

configurations in the two topologies, *anti* relative to each other in the α isomer and *syn* in the β isomer. Interconversion between the two isomers thus requires breaking of one Fe–N_{py} bond and the adjacent Fe–N_{amine} bond to allow one N-methyl group to epimerize. The inertness of the two isomers to interconversion provides us a unique opportunity to explore ligand topology effects on catalysis, and Tables 1 and 2 summarize our surprising results.

Table 1. Alkane oxidation reactivities of nonheme iron catalysts.[a]

	Fe(tpa)[b]	α-**1**	β-**1**	Fe(6-Me$_3$-tpa)[b]
cyclohexane				
A + K[c] (TN)[d]	3.2	5.9	1.9	1.4
[A]/[K]	5	9	0.9	1
KIE[e]	3.5	3.2	4.0	3.3
[$H_2{}^{18}O_2$/$H_2{}^{18}O$] (%)[f]	70/27	82/15	34/10	22/1
adamantane 3°/2°[g]	17	15	17	15
cis-DMCH[h] %RC[i]	> 99 %	> 99 %	68 %	54 %

[a] Reaction conditions: 0.7 mM catalyst, 7 mM H_2O_2, and 0.7 M substrate in CH_3CN at room temperature in air. H_2O_2 solution added by syringe pump over a 30-min period. [b] Data from references [5] and [6]. [c] A + K = alcohol + ketone. [d] TN = Turnover number. [e] KIE = Intermolecular kinetic isotope effect obtained from the competitive oxidation of *c*-C_6H_{12}/*c*-C_6D_{12} to cyclohexanol. [f] ^{18}O incorporated into cyclohexanol when $H_2{}^{18}O_2$ was used as a oxidant/when reaction was carried out in presence of 1000 equiv of $H_2{}^{18}O$. Other conditions as stated in [a]. [g] 3 × [1-adamantanol]/([2-adamantanol] + [2-adamantanone]). [h] DMCH = 1,2-dimethylcyclohexane. [i] %RC = 100 × (*cis*-*trans*)/(*cis* + *trans*).

Table 2. Olefin oxidation reactivities of nonheme iron catalysts.[a]

	Fe(tpa)[b]	α-**1**	β-**1**	Fe(6-Me$_3$-tpa)[b]
cyclooctene				
diol + epoxide (TN)[c]	7.4	6.5	7.7	5.6
[diol]/[epoxide]	1.2:1	0.1:1	1.8:1	7.0:1
epoxide %^{18}O [$H_2{}^{18}O_2$/$H_2{}^{18}O$](%)[d]	90/9	90/11	66/15	54/3
diol %^{18}O from $H_2{}^{18}O_2$ [noO/1O/2O](%)[e]	0/97/3	3/89/7	2/4/93	4/96
$H_2{}^{18}O$ [noO/1O/2O](%)[f]	13/86/1	11/88/1	97/3/0	99/1/0
cis-2-heptene				
diol + epoxide (TN)[c]	4.9	7.0	6.8	4.5
[diol]/[epoxide]	1.6:1	0.1:1	0.8:1	10:1
%RC[g] epoxide	80	> 99	67	35
%RC[g] diol	96	> 99	85	93
trans-2-heptene				
diol + epoxide (TN)[c]	4.8	5.7	5.6	4.1
[diol]/[epoxide]	2.2:1	0.05:1	0.6:1	13:1
%RC[g] epoxide	> 99	> 99	86	> 99
%RC[g] diol	96	> 99	81	96
1-octene				
diol + epoxide (TN)[c]	7.5	6.4	4.7	5.8
[diol]/[epoxide]	2.0:1	0.2:1	2.1:1	18:1

[a] Reaction conditions: 0.7 mM catalyst, 7 mM H_2O_2, and 0.7 M substrate in CH_3CN at room temperature in air. H_2O_2 solution added by syringe pump over a 30-min period. [b] Data from references [5] and [6]. [c] TN = Turnover number [d] ^{18}O incorporated into cyclooctene epoxide when $H_2{}^{18}O_2$ was used as a oxidant/when reaction was carried out in presence of 1000 equiv of $H_2{}^{18}O$. Other conditions as stated in [a]. [e] Percentage of *cis*-cyclooctane-1,2-diol that contains no ^{18}O/1 ^{18}O atom/2 ^{18}O atom when $H_2{}^{18}O_2$ was used as a oxidant. Other conditions as stated in [a]. [f] Percentage of *cis*-cyclooctane-1,2-diol that contains no ^{18}O/1 ^{18}O atom/2 ^{18}O atom when reaction was carried out in presence of 1000 equiv of $H_2{}^{18}O$. Other conditions as stated in [a]. [g] %RC = 100 × (*cis*-*trans*)/(*cis* + *trans*).

The data demonstrate that α-**1** is an effective catalyst for hydrocarbon oxidation, converting as much as 70% of the H_2O_2 introduced into oxidized products. Its high catalytic reactivity thus resembles that displayed by the isostructural $[Fe^{II}(bpmen)(CH_3CN)_2]^{2+}$ (bpmen = *N*,*N*′-bis(2-pyridylmethyl)-*N*,*N*′-dimethyl-1,2-diaminoethane).[13, 14] Furthermore the oxidations can be highly stereoselective. For example, the hydroxylation of *cis*-1,2-dimethylcyclohexane to the corresponding tertiary alcohol affords only the epimer with *cis*-dimethyl groups. Similarly, the oxidation of *cis*- and *trans*-2-heptene affords the corresponding epoxides and *cis*-diols with no detectable loss of stereochemistry. These stereospecific transformations, together with the high alcohol/ketone ratio obtained for cyclohexane hydroxylation, demonstrate that substrate radicals, if formed in the course of oxidation, must be quite short-lived. Thus the catalytic reactivity of α-**1** strongly parallels that of $[Fe^{II}(tpa)(CH_3CN)_2]^{2+}$ (**2**, tpa = tris(2-pyridylmethylamine)).[5–7]

Isotope-labeling experiments with $H_2{}^{18}O_2$ and $H_2{}^{18}O$ further establish the mechanistic similarity between α-**1** and **2** (Table 1 and Table 2). For cyclohexane hydroxylation and cyclooctene epoxidation carried out in the presence of H_2O, the oxygen atoms of the alcohol and epoxide products derive mainly from H_2O_2, with the balance from H_2O; little or no incorporation from O_2 is observed. Even more striking is the labeling pattern for the minor *cis*-dihydroxylation product of cyclooctene; the diol obtained from α-**1**, like that from **2**, derives one oxygen atom from H_2O_2 and the other from H_2O. These observations support the mechanism shown in Scheme 2 (left branch) invoking a low-spin Fe^{III}–OOH intermediate and a *cis*-HO–Fe^{V}=O oxidant derived therefrom; this mechanism previously proposed for **2** also accounts for all the mechanistic evidence for α-**1**.[5–7]

The oxidation behavior of β-**1** is significantly different from that of α-**1**. For this catalyst, there is strong evidence for the participation of longer lived radicals (Table 1 and Table 2): the low alcohol/ketone ratio for cyclohexane hydroxylation, the loss of stereochemistry in the oxidations of *cis*-1,2-

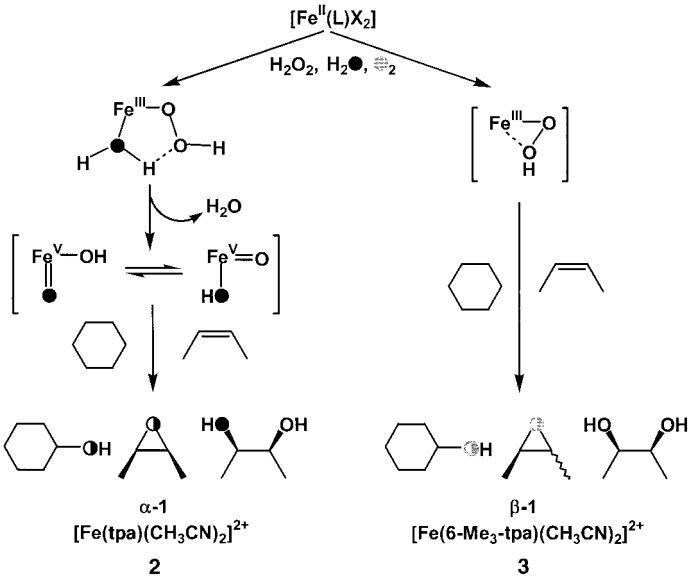

Scheme 2. Proposed mechanisms for the oxidations.

  1433-7851/02/4112-2180 $ 20.00+.50/0 *Angew. Chem. Int. Ed.* **2002**, *41*, No. 12

dimethylcyclohexane and *cis*-2-heptene, and the significant incorporation of O_2 into the alcohol and epoxide products. Such catalytic behavior strongly resembles that of $[Fe^{II}(6\text{-}Me_3\text{-tpa})(CH_3CN)_2]^{2+}$ (**3**).[5–7] Perhaps even more compelling is the catalysis of *cis*-dihydroxylation by β-**1**. Not only are the *cis*-diol/epoxide ratios increased by six- to tenfold relative to those observed for α-**1**, but the cyclooctene *cis*-dihydroxylation product also derives both oxygen atoms from H_2O_2, as reported for **3**.[4, 6]

Our results show that the small change in ligand topology around the metal center between α-**1** and β-**1** elicits dramatically distinct outcomes in the hydrocarbon oxidation reactions observed for these two isomers, ones that parallel the contrasting behavior of **2** and **3**. The difference between **2** and **3** is less subtle; **3** has 6-Me substituents whose steric effects affect the spin state of the Fe^{III}–OOH intermediate,[15] which in turn influences the course of the oxidations (Scheme 2, right branch).[5–7] By analogy, we propose that the distinct ligand topologies of α-**1** and β-**1** give rise to different spin states for their respective Fe^{III}–OOH intermediates. That the α-ligand topology exerts a stronger crystal field is clearly manifested in ^1H NMR experiments on the Fe^{II} catalysts in CD_3CN. While both isomers exhibit large paramagnetic shifts at 25 °C indicative of high-spin metal centers (Figure 1), the α isomer undergoes a transition to a diamagnetic low-spin form as it is cooled to -45 °C, indicated by a spectrum that spans only 12 ppm. In contrast, the β isomer remains high spin at -45 °C.

In summary, ligand effects appear to play a significant role in determining the course of hydrocarbon oxidation by nonheme iron catalysts in combination with H_2O_2. One important factor is the availability of two *cis*-labile sites as demonstrated by Chen et al.[5, 6] in a comparison of related tetradentate and pentadentate ligands and by Mekmouche et al.[16] in a comparison of $[Fe(L)X_2]$ (X = Cl or CH_3CN) catalysts. We have also shown the dramatic effect of introducing 6-methyl substituents on pyridine ligands.[5–7] Herein, we show that the catalytic chemistry can be controlled by ligand topology. This work demonstrates that exquisite tuning of the reaction mechanisms can be accomplished by subtle control of the coordination environment of the nonheme iron site. Such fine tuning may also serve as a precedent to understand the diversity on the reactions of hydrocarbon oxidation catalyzed by nonheme iron enzymes.

Experimental Section

β-$[Fe^{II}(bpmcn)(CF_3SO_3)_2]$ (β-**1**) was prepared as previously described.[8]

α-$[Fe^{II}(bpmcn)(CF_3SO_3)_2]$ (α-**1**) was prepared from α-$[Fe^{II}(bpmcn)Cl_2]$. Overnight reaction of bpmcn (1.63 g, 5 mmol) in CH_3CN (7 mL) with a vigorously stirred suspension of $FeCl_2$ (0.64 g, 5 mmol) in CH_3CN (3 mL) afforded a yellow precipitate that was filtered, washed with CH_3CN and dried under vacuum to afford the product α-$[Fe^{II}(bpmcn)Cl_2]$ (1.97 g; 87 %). Elemental analysis calcd (%) for $C_{20}H_{28}Cl_2FeN_4 \cdot H_2O$: C 51.19, H 6.44, N 11.94; found: C 51.38, H 6.20, N 12.21. A suspension of α-$[Fe^{II}(bpmcn)Cl_2]$ (800 mg, 1.78 mmol) in CH_3CN (5 mL) was then treated with a solution of $AgCF_3SO_3$ (912 mg, 3.55 mmol) in CH_3CN (4 mL), resulting in the formation of a fine precipitate of AgCl, which was filtered away after allowing the mixture to stir. The filtrate was then dried in vacuo, yielding the desired complex as a pale yellow powder. Recrystallization from CH_2Cl_2/diethyl ether afforded α-**1** as large pale yellow blocks (1.19 g, 99 %). Elemental analysis calcd (%) for $C_{22}H_{28}F_6FeN_4O_6S_2$: C 38.95, H 4.16, N 8.26, S 9.45; found: C 38.97, H 4.37, N 8.30, S 9.41.

Received: January 16, 2002
Revised: March 19, 2002 [Z18530]

[1] L. Que, Jr., R. Y. N. Ho, *Chem. Rev.* **1996**, *96*, 2607 – 2624.
[2] E. I. Solomon, T. C. Brunold, M. I. Davis, J. N. Kemsley, S.-K. Lee, N. Lehnert, F. Neese, A. J. Skulan, Y.-S. Yang, J. Zhou, *Chem. Rev.* **2000**, *100*, 235 – 349.
[3] C. Kim, K. Chen, J. Kim, L. Que, Jr., *J. Am. Chem. Soc.* **1997**, *119*, 5964 – 5965.
[4] K. Chen, L. Que, Jr., *Angew. Chem.* **1999**, *111*, 2365—2368; *Angew. Chem. Int. Ed.* **1999**, *38*, 2227 – 2229.
[5] K. Chen, L. Que, Jr., *J. Am. Chem. Soc.* **2001**, *123*, 6327 – 6337.
[6] K. Chen, M. Costas, J. Kim, A. K. Tipton, L. Que, Jr., *J. Am. Chem. Soc.* **2002**, *124*, 3026 – 3035.
[7] K. Chen, M. Costas, L. Que, Jr., *J. Chem. Soc. Dalton Trans.* **2002**, 672 – 679.
[8] M. Costas, A. K. Tipton, K. Chen, D.-H. Jo, L. Que, Jr., *J. Am. Chem. Soc.* **2001**, *123*, 6722 – 6723.
[9] J. R. Aldrich-Wright, R. S. Vagg, P. A. Williams, *Coord. Chem. Rev.* **1997**, *166*, 361 – 389.
[10] U. Knof, A. von Zelewsky, *Angew. Chem.* **1999**, *111*, 312—333; *Angew. Chem. Int. Ed.* **1999**, *38*, 302 – 322.
[11] C. Ng, M. Sabat, C. L. Fraser, *Inorg. Chem.* **1999**, *38*, 5545 – 5556.
[12] M. Costas, J.-U. Rohde, A. Stubna, R. Y. N. Ho, L. Quaroni, E. Münck, L. Que, Jr., *J. Am. Chem. Soc.* **2001**, *123*, 12931 – 12932.
[13] K. Chen, L. Que, Jr., *Chem. Commun.* **1999**, 1375 – 1376.
[14] M. C. White, A. G. Doyle, E. N. Jacobsen, *J. Am. Chem. Soc.* **2001**, *123*, 7194 – 7195.
[15] Y. Zang, J. Kim, Y. Dong, E. C. Wilkinson, E. H. Appelman, L. Que, Jr., *J. Am. Chem. Soc.* **1997**, *119*, 4197 – 4205.
[16] Y. Mekmouche, S. Ménage, C. Toia-Duboc, M. Fontecave, J.-B. Galey, C. Lebrun, J. Pecaut, *Angew. Chem.* **2001**, *113*, 975—978; *Angew. Chem. Int. Ed.* **2001**, *40*, 949 – 952.

Design of a Bilayer Structure in an Organic Inclusion Compound**

Sang-Ok Lee, Benson M. Kariuki, and Kenneth D. M. Harris*

Since their discovery over 50 years ago,[1, 2] several hundreds of urea inclusion compounds[3–11] have been prepared containing different types of guest molecules (mainly based on *n*-alkane chains, with only a limited degree of substitution allowed). The vast majority of urea inclusion compounds are based on a hexagonal host structure[3, 12] that comprises continuous, parallel tunnels constructed from a hydrogen-bonded arrangement of urea molecules. These "conventional"

[*] Prof. Dr K. D. M. Harris, Dr S.-O. Lee, Dr B. M. Kariuki
School of Chemical Sciences
University of Birmingham
Edgbaston, Birmingham B15 2TT (United Kingdom)
Fax: (+44) 121-414-7473
E-mail: K.D.M.Harris@bham.ac.uk

[**] We are grateful to the EPSRC, the University of Birmingham, and CVCP for financial support.

  1433-7851/02/4112-2181 $ 20.00+.50/0